V European Conference on Computational Fluid Dynamics
ECCOMAS CFD 2010
J. C. F. Pereira and A. Sequeira (Eds)
Lisbon, Portugal,14-17 June 2010

A CONSISTENT REGULARIZATION OF THE INCOMPRESSIBLE NAVIER–STOKES EQUATIONS VIA COMPUTATION OF THE VORTICITY

Mika Malinen*

*CSC – IT Center for Science Ltd.
P.O. Box 405, FI-02101 Espoo, Finland
e-mail: mika.malinen@csc.fi

Key words: incompressible flow, finite element, stabilized method, rotational form, pressure Poisson equation

Abstract. *An alternate formulation of the pressure Poisson equation expressed using the velocity and vorticity variables is employed to obtain a variationally consistent regularization of the incompressible Navier–Stokes equations. A discrete version of the regularized system leads to a stabilized finite element formulation which may be discretized conveniently using equal-order interpolation elements. In this paper, the usefulness of the finite element formulation is demonstrated experimentally in connection with the rotational form of the Navier–Stokes system, where the ability to resolve the associated pressure variable more accurately than possible by using standard mixed-interpolation elements may be particularly beneficial. The experimental results obtained by using test problems that have known exact solutions show that the optimal orders of convergence are reached for a large range of stabilization parameter values. The robustness with respect to variations of other problem or discretization parameters, such as the Reynolds number and the time step, is also illustrated. In addition, benchmark computations in the case of flow over a cylinder show that enabling equal-order interpolation via the stabilization is a practical alternative to alleviate the deficiency of certain mixed-interpolation elements to produce qualitatively correct flow features, such as vortex shedding, on coarse meshes.*

1 INTRODUCTION

Consider finding the velocity $\mathbf{v}'(\mathbf{x}', t')$ and pressure $p'(\mathbf{x}', t')$ governed by the incompressible Navier-Stokes equations

$$\begin{aligned} S\frac{\partial \mathbf{v}'}{\partial t'} + (\mathbf{v}' \cdot \nabla')\mathbf{v}' - \frac{1}{Re}\Delta'\mathbf{v}' + E\nabla' p' = \mathbf{f}' \quad \text{in } \Omega' \times (0, T'), \\ \nabla' \cdot \mathbf{v}' = 0 \quad \text{in } \Omega' \times (0, T'), \end{aligned} \tag{1}$$

which have been made dimensionless by introducing the scaled variables

$$\mathbf{x}' = \frac{\mathbf{x}}{L}, \quad t' = \frac{t}{T}, \quad \mathbf{v}' = \frac{\mathbf{v}}{V}, \quad p' = \frac{p}{p_0}. \tag{2}$$

Here L and T define the length and time scales, V and p_0 are typical values of the velocity and pressure, ideally chosen such that $\mathbf{v}' \sim p' = O(1)$, while the Strouhal number S, the Reynolds number Re and the Euler number E are expressed in terms of the characteristic values as

$$S = L/(TV), \quad Re = \rho V L/\mu, \quad E = p_0/(\rho V^2), \tag{3}$$

with μ and ρ the fluid viscosity and density.

An alternate formulation of the Navier–Stokes system is obtained by expressing the convection term in the rotational form.[1] The field equations corresponding to this formulation may be written as

$$\begin{aligned} S\frac{\partial \mathbf{v}'}{\partial t'} + \boldsymbol{\omega}' \times \mathbf{v}' - \frac{1}{Re}\Delta'\mathbf{v}' + \nabla' P' = \mathbf{f}', \\ \boldsymbol{\omega}' - \nabla' \times \mathbf{v}' = \mathbf{0}, \\ \nabla' \cdot \mathbf{v}' = 0, \end{aligned} \tag{4}$$

where

$$P' = Ep' + \frac{1}{2}\mathbf{v}' \cdot \mathbf{v}' \tag{5}$$

is the dimensionless total pressure. In the following, we assume that mixed boundary conditions are imposed so that the velocity and the dimensionless surface traction $\mathbf{s}'$ are given on complementary parts as

$$\mathbf{v}' = \hat{\mathbf{v}} \text{ on } \Gamma'_D \tag{6}$$

and

$$\mathbf{s}' = (-P' + \frac{1}{2}\mathbf{v}' \cdot \mathbf{v}')\mathbf{n} + \frac{2}{Re}\mathbf{D}'(\mathbf{v}')\mathbf{n} = \mathbf{0} \text{ on } \Gamma'_N = \partial\Omega' \backslash \Gamma'_D. \tag{7}$$

Here $\mathbf{D}'(\mathbf{v}')$ is the symmetric part of the velocity gradient, and $\mathbf{n}$ is the outward unit normal vector to the boundary $\partial\Omega'$ of the d-dimensional body Ω'.

It is well known that the requirement of inf-sup stability[2] prevents the approximation of the standard weak formulation of the Navier–Stokes system (1) by using equal-order finite element expansions of both unknowns. However, equal-order interpolation elements that are very appealing from the viewpoint of computer implementation are enabled by using stabilized methods which employ regularization of the weak formulation. While there is now an extensive literature on stabilized methods for the incompressible Navier–Stokes equations in the standard convection form,[3] the subject of finite element approximation of the rotational form has gained less attention and remains to be exhausted.

Obviously, the requirement of inf-sup stability arises also when the rotational form is employed. Despite having formal similarity, inf-sup stable discretizations of the rotational form have been observed to display a less accurate error behavior than those of the standard convection form. As noted recently, this behavior may be explained, at least partially, by the fact that the total pressure solution is often more detailed than the standard pressure and hence inf-sup stable discretizations — which typically use a higher dimensional approximation for the velocity compared to that of the pressure variable — may leave the discrete total pressure inaccurate.[4] We note that such a disparity does not arise when the same approximation space is used for the discretization of both the velocity and total pressure, so utilizing stabilized methods seems to be especially well-suited for approximating the rotational form.

We note that in practice the computational solution of the rotational form as given by (4) does not necessitate taking the vorticity $\boldsymbol{\omega}'$ to be an additional unknown. However, nonstandard ways to approximate the system emerge when the vorticity is treated as an auxiliary variable. In particular, if the vorticity and divergence-free velocity are available and the solution generally has sufficient regularity, the pressure field associated with the incompressible flow equations can be generated using the weak formulation of a consistent pressure equation. In this study, we shall explore ways to utilize such a principle in the formulation of consistently stabilized methods. The regularization strategy we consider is described in Section 2. Then, in Section 3, computational convergence tests are performed in the case of both the stationary and evolutionary versions of the Navier–Stokes equations by utilizing manufactured solutions. The optimal orders of convergence which are demonstrated experimentally for large ranges of regularization parameter and other problem or discretization parameter values illustrate the potential of the method we propose.

Standard notation will be used. For brevity the L^2 inner product is denoted by $(\cdot,\cdot)$, with the domain of integration indicated using a subscript if different from Ω'. Similarly, the corresponding norm is denoted by $||\cdot||$.

2 A REGULARIZED FORMULATION

If the solution of the Navier–Stokes problem is so regular that

$$\begin{aligned} \mathbf{v}' &\in L^2(0,T';H^2(\Omega')^d)\cap H^1(0,T';L^2(\Omega')^d),\\ \nabla' P' &\in L^2(0,T';L^2(\Omega')^d), \end{aligned} \tag{8}$$

then, by noting that $-\Delta'\mathbf{v}' = \nabla' \times \nabla' \times \mathbf{v}' - \nabla'(\nabla' \cdot \mathbf{v}') = \nabla' \times \boldsymbol{\omega}'$, the solution is found to satisfy

$$(\nabla' P' + \boldsymbol{\omega}' \times \mathbf{v}' - \mathbf{f}', \nabla'\phi') + \frac{1}{Re}(\nabla' \times \boldsymbol{\omega}', \nabla'\phi') + (S\frac{\partial \mathbf{v}'}{\partial t'}, \nabla'\phi') = 0 \tag{9}$$

for any $\phi' \in H^1(\Omega')$. Thus, in view of (9), we may regularize the variational formulation of the problem by modifying the weak formulation of the incompressibility constraint as

$$\begin{aligned} -(\nabla' \cdot \mathbf{v}', \phi') - \epsilon(\nabla' P' + \boldsymbol{\omega}' \times \mathbf{v}' - \mathbf{f}', \nabla'\phi') - \frac{\epsilon}{Re}(\nabla' \times \boldsymbol{\omega}', \nabla'\phi') \\ - \epsilon(S\frac{\partial \mathbf{v}'}{\partial t'}, \nabla'\phi') = 0, \end{aligned} \tag{10}$$

where ϵ is a dimensionless parameter chosen to be so small that the incompressibility constraint is essentially respected.

We are thus led to considering the following regularized problem: Find $\mathbf{v}'(\cdot, t') \in X$, $\boldsymbol{\omega}'(\cdot, t') \in H^1(\Omega')$ and $P'(\cdot, t') \in H^1(\Omega')$ such that

$$\begin{aligned} (S\frac{\partial \mathbf{v}'}{\partial t'}, \mathbf{z}') + ((\nabla' \times \mathbf{v}') \times \mathbf{v}', \mathbf{z}') + \frac{2}{Re}(\mathbf{D}'(\mathbf{v}'), \mathbf{D}'(\mathbf{z}')) - (P', \nabla' \cdot \mathbf{z}') \\ +1/2(\mathbf{v}' \cdot \mathbf{v}', \mathbf{z}' \cdot \mathbf{n})_{\Gamma'_N} = (\mathbf{f}', \mathbf{z}'), \\ (\boldsymbol{\omega}', \boldsymbol{\eta}') - (\nabla' \times \mathbf{v}', \boldsymbol{\eta}') = 0, \\ -(\nabla' \cdot \mathbf{v}', \phi') - \epsilon(\nabla' P' + \boldsymbol{\omega}' \times \mathbf{v}' - \mathbf{f}', \nabla'\phi') - \frac{\epsilon}{Re}(\nabla' \times \boldsymbol{\omega}', \nabla'\phi') \\ -\epsilon(S\frac{\partial \mathbf{v}'}{\partial t'}, \nabla'\phi') = 0 \end{aligned} \tag{11}$$

for all $(\mathbf{z}', \boldsymbol{\eta}', \phi') \in Z \times H^1(\Omega') \times H^1(\Omega')$ and $t' \in (0, T')$. Here the velocity solution and test spaces X and Z are subsets of $H^1(\Omega')^d$ consisting of functions which on the part Γ'_D satisfy the constraints $\mathbf{v}' = \hat{\mathbf{v}}$ and $\mathbf{z}' = \mathbf{0}$, respectively. The variational consistency of the formulation (11) is emphasized; strong solutions with the supposed regularity (8) exactly satisfy the weak formulation (11).

Finite element approximations of the regularized problem can be obtained in a standard manner by replacing the infinite-dimensional spaces by chosen finite element spaces. Fully discrete approximation finally follows by time discretization. Our experimental observation is that the regularized formulation may be discretized in a stable way by using equal-order continuous approximations for all the unknowns. It also appears that the time-accuracy may be retained in a natural manner. We note that when $\epsilon = 0$, the velocity and pressure approximations are unaffected by the vorticity approximation, so in this case the same (possibly inf-sup deficient) approximations could also be obtained by using the discrete version of the rotational formulation in the velocity and total pressure variables.

Before turning to experimental results, we close this section by noting that the accuracy of the vorticity approximation is likely to be a critical factor so that the discrete version of (9) is useful. In the lowest-order case the finite element approximation of $\nabla' \times \boldsymbol{\omega}'$ may not be convergent and using a mesh-dependent regularization parameter may therefore be necessary in order to ensure the asymptotic convergence of the stabilized finite element solution.

3 EXPERIMENTAL RESULTS

In this section, convergence of the regularized scheme based on equal-order elements is explored experimentally. First, the asymptotic order of convergence is studied in the case of the steady version of the Navier–Stokes equations on a two-dimensional domain Ω. The question of an optimal choice of the stabilization parameter ϵ is also considered in this setting. The convergence of the evolutionary version is explored after this.

In the following, the order of piecewise polynomial approximation and the dimensionless length of the longest edge in the mesh will be denoted by m and h, respectively. Our intention here is to keep errors arising from the nonlinear iteration small by using a stringent convergence tolerance. Therefore, the nonlinear iteration is terminated when the ratio of the vector 2-norm of the nonlinear residual to the right-hand side 2-norm is less than 10^{-10}.

3.1 Convergence of the steady-state version: quadratic approximation

To begin with we consider the steady Navier–Stokes problem for which the solution is

$$\begin{aligned} v_1 &= \frac{p_0 L}{\mu} \sin(\frac{x_1}{L}) \sin(\frac{x_2}{L} + 1), \\ v_2 &= \frac{p_0 L}{\mu} \cos(\frac{x_1}{L}) \cos(\frac{x_2}{L} + 1), \\ p &= 2p_0 \cos(\frac{x_1}{L}) \sin(\frac{x_2}{L} + 1) \end{aligned} \tag{12}$$

on $\Omega = (0, L) \times (0, L)$. This manufactured solution satisfies a zero traction condition on the boundary $x_1 = 0$. We now take $L = 1$, $\rho = 1$, $p_0 = 1$, and $V = p_0 L/\mu$. Then, given the viscosity μ, we have $Re = 1/\mu^2$ and $E = 1/Re$. In addition, the components of the body force vector are accordingly taken to be

$$\begin{aligned} f_1' &= \sin(x_1') \cos(x_1'), \\ f_2' &= (2/Re + 2E) \cos(x_1') \cos(x_2' + 1) - \cos(x_2' + 1) \sin(x_2' + 1). \end{aligned} \tag{13}$$

We focus here on the use of quadratic approximation, i.e. we take $m = 2$. Also, we start by considering the convergence of the regularized scheme when $Re = 1$. In this case the viscous, convective and pressure terms all have the same order of magnitude, so observing an optimal asymptotic convergence as the mesh size h decreases is likely to indicate that all terms in the discrete Navier–Stokes problem are resolved with optimal accuracy.

In Figure 1 we display the L^2 norms of the errors of velocity and total pressure approximations on a sequence of nonstructured triangular meshes. In this experiment uniform meshes are used, and the stabilization parameter is varied as $\epsilon = h^k/100$, with $k = 0, 1, 2$. We see that especially the error of the pressure is sensitive with respect to the order of the h-scaling of the stabilization parameter. For the choice $\epsilon = h/100$ the velocity and pressure errors both are $O(h^3)$ and thus show optimal accuracy. When $\epsilon = 1/100$, the asymptotic errors appear to be $O(h^2)$. Importantly, although this convergence order is not optimal, over-stabilization by neglecting the h-dependent weight in the regularization parameter does not thus sacrifice the asymptotic validity of the computational model as $h \to 0$.

The sensitivity with respect to a change of the stabilization parameter is explored further in Figure 2 where the total pressure error is shown for the choice $\epsilon = C_\epsilon h$, with C_ϵ being a parameter. We have $\max(C_\epsilon)/\min(C_\epsilon) = 20$ for the values used in the experiment and yet the pressure error is more or less the same (it is noted that the velocity error, which is not shown, remains essentially unaffected by these variations). The robustness observed suggests also that when nonuniform meshes are employed, using a "right" mesh size h in the expression of the stabilization parameter may not be excessively important for the performance.

Obviously, using uniform meshes is unrealistic in practice. Although the experiments given so far demonstrate that the error behavior is not very sensitive with respect to the choice of the stabilization parameter, a concern arises whether associating the mesh size h with the longest edge in the mesh leads to over-stabilization and non-optimal accuracy in regions where the mesh size is considerably smaller. For example, in a realistic case, one may be interested in computing the surface traction on a boundary to a high accuracy, while a less fine mesh may be used in other parts where a high resolution is not of an interest. To imitate such a situation, we now consider three meshes which all have $h = 1/5$ and which are refined towards the edge where the vanishing surface traction condition is imposed. The discretization mesh size on the traction boundary is taken to be $h_K = 1/50$, $1/100$ and $1/200$, so that the ratio of the longest element edge to the shortest element edge on the mesh varies as $\theta = 10, 20, 40$. In Table 1 we give the vector 2-norm of the total contact force $\mathbf{t}$ exerted on the boundary $x_1 = 0$ when the constant stabilization parameter $\epsilon = 5h/1000$ is used. We see that the total force is $O(h_K^2)$ which is a locally optimal behavior as the computation of the surface force requires evaluating the velocity gradient.

	$\theta = 10$	$\theta = 20$	$\theta = 40$
$\lvert\mathbf{t}\rvert$	4.6689E-06	1.1420E-06	2.8068E-07
$\lvert\lvert\mathbf{v}' - \mathbf{v}'_h\rvert\rvert$	1.2052E-05	8.7003E-06	1.2227E-05
$\lvert\lvert P' - P'_h\rvert\rvert$	9.8013E-05	5.9788E-05	1.2898E-04

Table 1: The vector 2-norm of the contact force $\mathbf{t}$ and the L^2 norms of the velocity and total pressure errors when a mesh of grading degree θ is used.

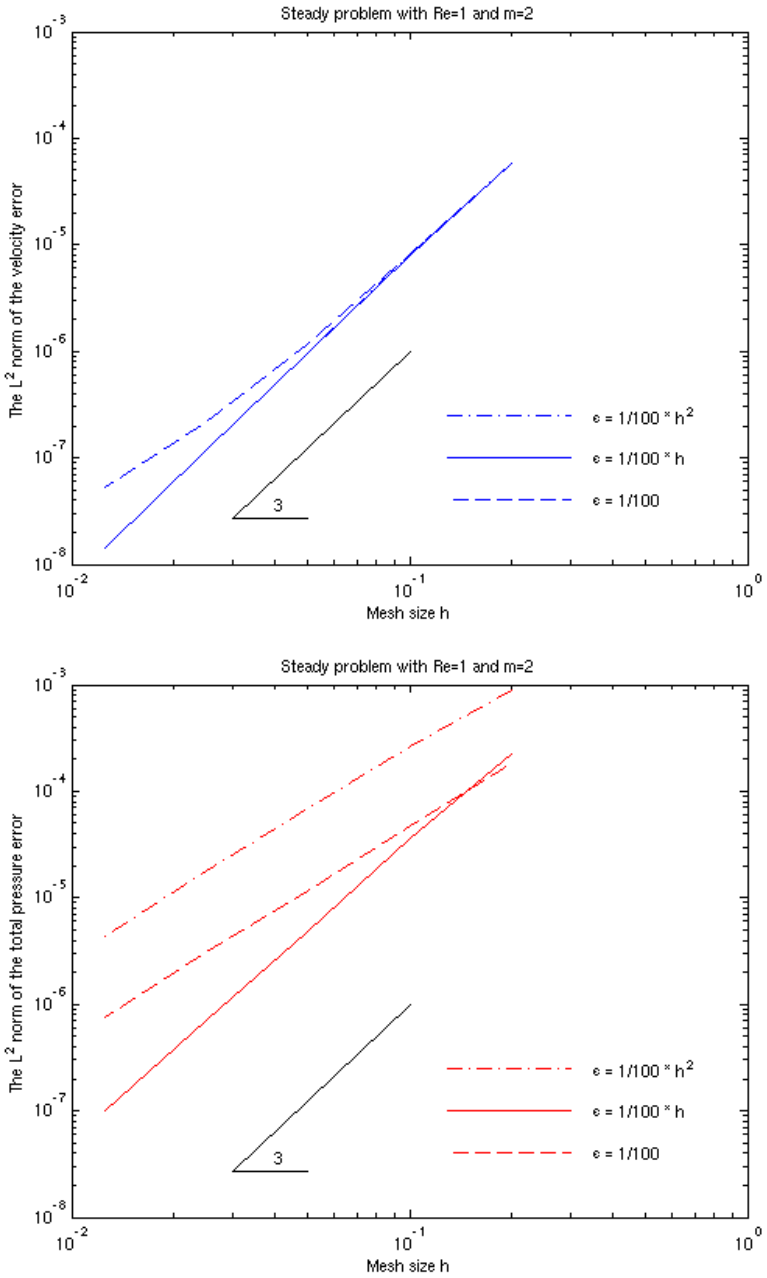

Figure 1: The L^2 norms of the velocity and total pressure errors in the case of the steady problem for $Re = 1$. The stabilization parameter is varied as $\epsilon = h^k/100$, $k = 0, 1, 2$, and $m = 2$.

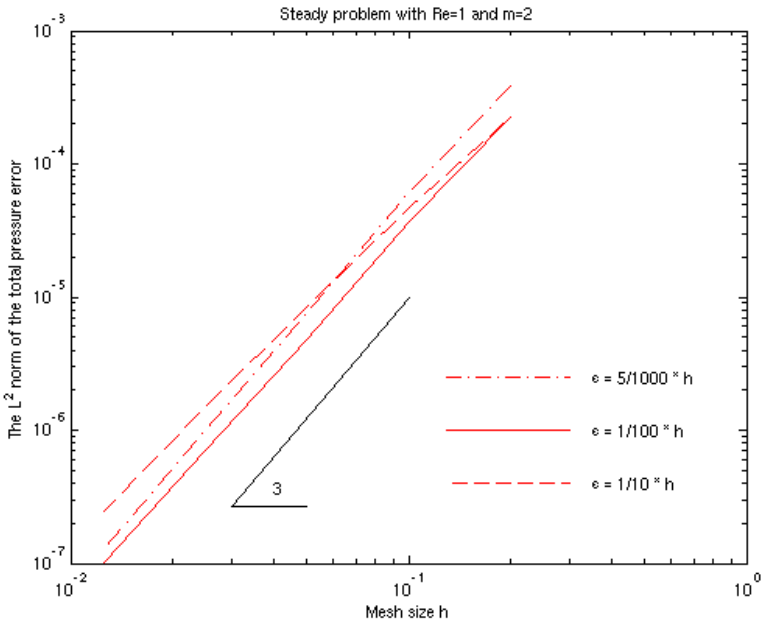

Figure 2: The sensitivity of the total pressure error ($m = 2$) with respect to the value of the stabilization parameter in the case of the steady problem for $Re = 1$.

Finally, the robustness with respect to variations of the Reynolds number is illustrated in Figure 3 where the L^2 norms of the total pressure and velocity errors on a sequence of uniform meshes are displayed for $Re = 1$ and $Re = 100$. We see that both the errors are essentially unaffected by the Reynolds number. An increasing error of the standard pressure approximation p'_h obtained by a post-processing computation

$$p'_h = \frac{1}{E}(P'_h - \frac{1}{2}\mathbf{v}'_h \cdot \mathbf{v}'_h) = Re(P'_h - \frac{1}{2}\mathbf{v}'_h \cdot \mathbf{v}'_h) \tag{14}$$

was nevertheless observed. Indeed, (14) implies that when the Euler number decreases, smaller errors in $\mathbf{v}'_h$ and P'_h are required in order to obtain the same accuracy of p'_h .

3.2 Convergence of the steady-state version: linear approximation

In this section we repeat some of the convergence tests when linear approximation is used, i.e. we now take $m = 1$. First, Figure 4 displays results corresponding to an experiment similar to that which is considered in Figure 1. For reference we also show the velocity and total pressure errors when the rotational form of the Navier-Stokes system in the velocity and pressure variables is discretized using the MINI finite element. We see that the approximations of the velocity and pressure are again optimally convergent with order $m+1$ when the regularization parameter is scaled using the weight h. Furthermore, an additional test showed that a slightly better convergence was again possible if the

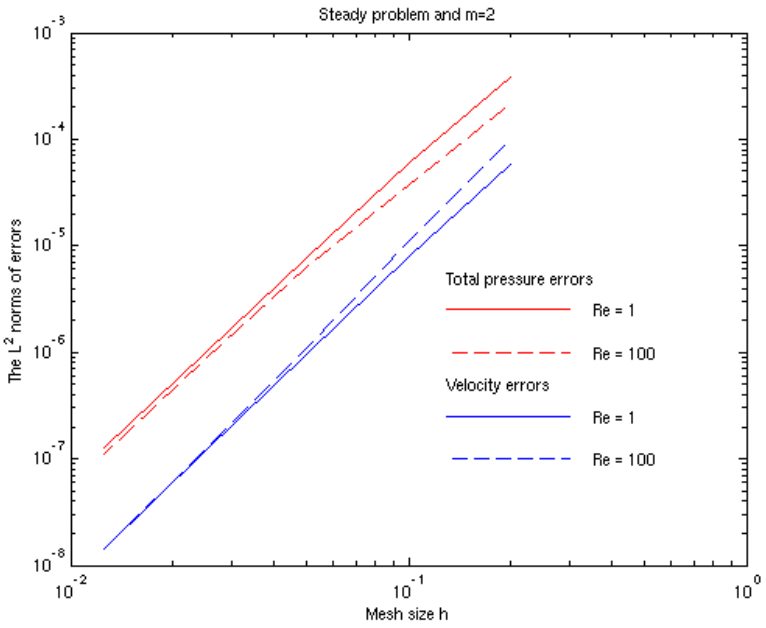

Figure 3: The sensitivity of the total pressure and velocity errors ($m = 2$ and $\epsilon = 5h/1000$) with respect to variations of the Reynolds number.

regularization parameter was taken to be $\epsilon = 5h/1000$ instead of the value $\epsilon = h/100$. We note that the MINI element and the regularized scheme with the choice $\epsilon = h^2/100$ display more or less the same error behavior with the error of the pressure being $O(h^{3/2})$. It is also noted that the poor behavior seen in the case of $\epsilon = 1/100$ is expected as the approximation of $\nabla' \times \boldsymbol{\omega}'$ may not be convergent in the case of linear approximation.

The sensitivity with respect to a change of the Reynolds number is explored in Figure 5. Interestingly, the quality of the total pressure approximation improves clearly as the Reynolds number increases. This behavior may be explained by the fact that the relative importance of the poorly resolved stabilization term depending on $\nabla' \times \boldsymbol{\omega}'_h$ diminishes for larger Reynolds numbers.

3.3 Convergence of the evolutionary version

We now consider the time-dependent problem for which the solution is

$$\begin{aligned} v_1 &= \frac{p_0 L}{\mu} \sin(\frac{x_1}{L}) \sin(\frac{x_2}{L} + \frac{t}{T}), \\ v_2 &= \frac{p_0 L}{\mu} \cos(\frac{x_1}{L}) \cos(\frac{x_2}{L} + \frac{t}{T}), \\ p &= 2p_0 \cos(\frac{x_1}{L}) \sin(\frac{x_2}{L} + \frac{t}{T}) \end{aligned} \tag{15}$$

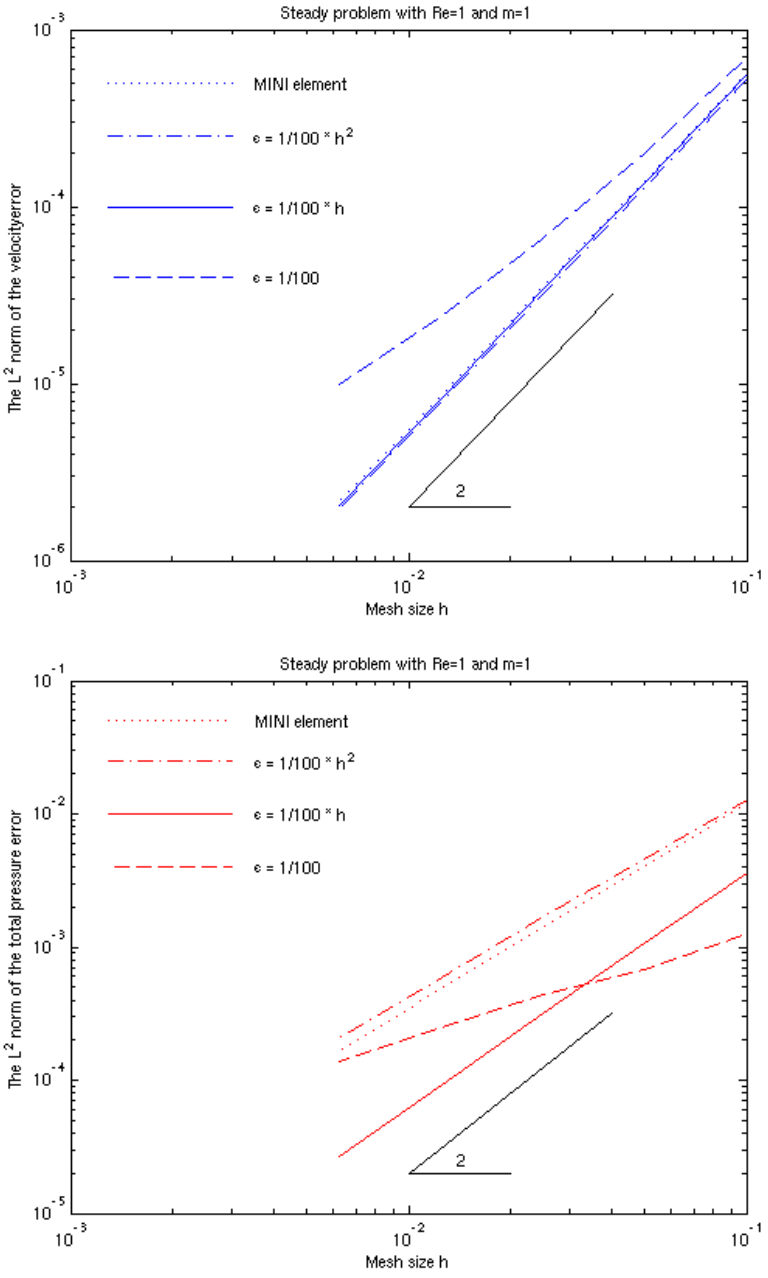

Figure 4: The L^2 norms of the velocity and total pressure errors in the case of the steady problem when $Re = 1$ and $m = 1$. The stabilization parameter for the regularized method is varied as $\epsilon = h^k/100$, $k = 0, 1, 2$.

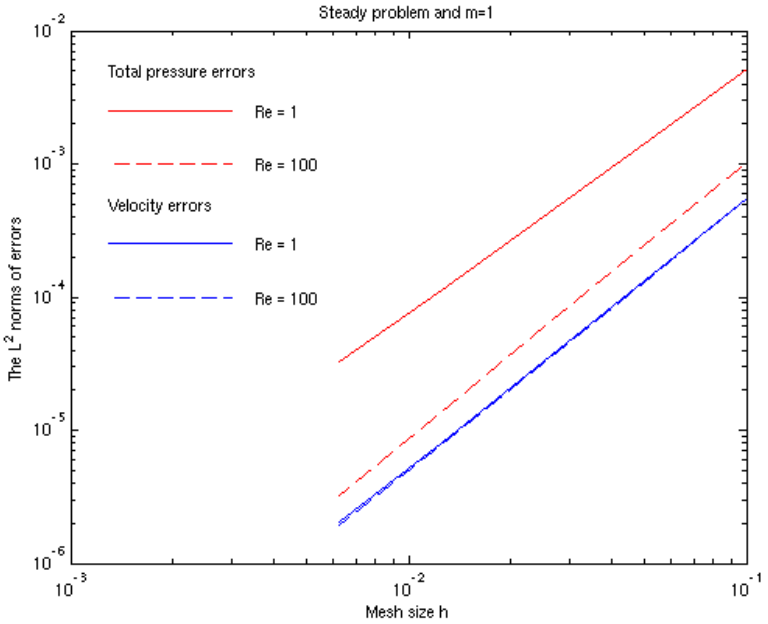

Figure 5: The sensitivity of the total pressure and velocity errors ($m = 1$ and $\epsilon = 5h/1000$) with respect to variations of the Reynolds number.

on $\Omega = (0, L) \times (0, L)$. In analogy to the steady state problem, the zero traction boundary condition is satisfied on the edge $x_1 = 0$. Here we set $T = 1$ and again take $L = 1$, $\rho = 1$, $p_0 = 1$, and $V = p_0 L/\mu$. The Reynolds number and the Euler number are then defined as for the steady problem, and the Strouhal number is expressed in terms of the viscosity as $S = \mu$. Also, the components of the body force are given by

$$\begin{aligned} f_1' &= S \sin(x_1') \cos(x_2' + t') + \sin(x_1') \cos(x_1'), \\ f_2' &= -S \cos(x_1') \sin(x_2' + t') + (2/Re + 2E) \cos(x_1') \cos(x_2' + t') \\ &\quad - \cos(x_2' + t') \sin(x_2' + t'). \end{aligned} \tag{16}$$

We note that the instantaneous solution at $t' = 1$ is the same as the steady state solution considered in the convergence study of the steady version.

For the time discretization the fully implicit BDF(2) is used. Throughout the experiments considered in the following, we use the stabilization parameter $\epsilon = 5h/1000$ and take $m = 2$. To begin with, we verify that the added stabilization terms do not have an effect on the time accuracy. To demonstrate this, we use a uniform mesh with $h = 1/40$ and employ time steps satisfying $\Delta t' \leq 1/80$. In this regime the velocity and total pressure errors are dominated by the spatial discretization error. The velocity and total pressure errors at $t' = 1$ which are recorded in Table 2 show that both the errors are of order 2. That is, we see the expected behavior that when $\Delta t'$ is halved, the error decreases by a factor of about 4.

	$\Delta t' = 1/10$	$\Delta t' = 1/20$	$\Delta t' = 1/40$	$\Delta t' = 1/80$
$\|\|\mathbf{v}' - \mathbf{v}'_h\|\|$	2.9592E-05	7.4450E-06	1.8693E-06	4.8136E-07
$\|\|P' - P'_h\|\|$	7.5811E-04	1.8989E-04	4.7517E-05	1.1925E-05

Table 2: The L^2 norms of the velocity and total pressure errors at $t' = 1$ for different time step sizes ($h = 1/40$ and $m = 2$).

Next we use a small time step so that the errors become dominated by the spatial discretization. The L^2 norms of the velocity and total pressure errors given in Table 3 for $\Delta t' = 1/320$ show that both approximations are again optimally convergent with order $m + 1$. Thus, the order of convergence with respect to the spatial discretization appears to be optimal for both the steady and evolutionary versions of the equations when the stabilization parameter is taken to be

$$\epsilon = \frac{5}{1000} h. \tag{17}$$

Importantly, it also appears that using very small time steps does not produce any anomalies of the type reported in the related literature on stabilized finite element methods.[5] If we take $h = 1/5$ and $\Delta t' = 1/2560$, the L^2 norms of the velocity and total pressure errors are $5.8096 \cdot 10^{-5}$ and $3.8742 \cdot 10^{-4}$, respectively, which agree with the corresponding values given in Table 3 to four digits even though the ratio $h^2/\Delta t'$ is as large as 102.4.

	$h = 1/5$	$h = 1/10$	$h = 1/20$	$h = 1/40$
$\|\|\mathbf{v}' - \mathbf{v}'_h\|\|$	5.8096E-05	8.0320E-06	9.5359E-07	1.2047E-07
$\|\|P' - P'_h\|\|$	3.8741E-04	6.0984E-05	7.6548E-06	1.2522E-06

Table 3: The L^2 norms of the velocity and total pressure errors at $t' = 1$ when $\Delta t' = 1/320$, $m = 2$ and a sequence of uniformly refined meshes is used.

3.4 Flow around a cylinder

To demonstrate the utility of the ideas further, we finally consider a more realistic problem setup and show that the regularization terms may enhance substantially the quality of a discrete solution already on a coarse mesh. The problem we consider is a standard benchmark case of two-dimensional flow over a circular cylinder.[6] The computational domain is given by $\Omega = (0, 2.2 \text{ m}) \times (0, H) \setminus \Omega_C$, where $H = 0.41$ m and the boundary of the body Ω_C is a circle having the diameter $D = 0.1$ m and the center point at $\mathbf{x}$=(0.2m,0.2m). On the inflow boundary $x_1 = 0$ a flow profile with components

$$\begin{aligned} v_1 &= 6 \sin(\pi t/8)(1 - x_2/H)x_2/H \quad (\text{m/s}), \\ v_2 &= 0 \end{aligned} \tag{18}$$

is prescribed, while on the outflow boundary $x_1 = 2.2$ m the normal component of the surface traction and the tangential velocity are assumed to vanish. A zero velocity condition is imposed at the top and bottom of the channel. In addition, the fluid density and viscosity are given by $\rho = 1$ kg/m^3 and $\mu = 0.001$ kg/(ms).

It has been demonstrated in a recent study[4] that a computational model based on the rotational form discretized by using standard inf-sup stable finite elements may fail to produce a discrete solution which reproduces a characteristic vortex shedding phenomenon associated with the flow problem. As noted therein, the failure may be explained, at least partially, by the fact that the total pressure solution is basically as detailed as the velocity solution and hence inf-sup stable discretizations, which typically use a higher dimensional approximation for the velocity compared to that of the pressure, may leave the discrete total pressure inaccurate. Obviously, such a disparity is naturally avoided when the same approximation space is used for the discretization of the velocity and total pressure.

In Figure 6 a coarse mesh approximation of the total pressure at $t = 5$ obtained by using inf-sup stable $P2P1$ approximation of the rotational form in the velocity and pressure variables is compared with the regularized solution defined on the same triangulation with $m = 2$. The contour plots shown illustrate that $P2P1$ approximation indeed fails to reproduce the von Karman vortex street, while the regularized scheme is able to produce the vortex shedding phenomenon. We note that in both simulations the fully implicit BDF(2) time-stepping with the time step $\Delta t = 0.005$ was employed. It should also be noted that the dimensionless equations were not employed here. In particular, the equation (10) may be expressed in terms of the dimensional variables as

$$-(\nabla \cdot \mathbf{v}, \phi)_\Omega - \varepsilon(\rho \frac{\partial \mathbf{v}}{\partial t} + \rho \boldsymbol{\omega} \times \mathbf{v} + \mu \nabla \times \boldsymbol{\omega} + \nabla P - \mathbf{f}, \nabla \phi)_\Omega = 0, \tag{19}$$

where

$$\varepsilon = \frac{L}{\rho V} \epsilon. \tag{20}$$

Here $V = V(t)$ was taken to be the maximum flow speed on the inflow boundary and the dimensionless parameter ϵ was defined as in (17).

4 CONCLUDING REMARKS

The pressure Poisson equation formulations have traditionally been employed to develop sequential solution methods[1,7] for the incompressible Navier–Stokes equations and, also, to recover the pressure solution in connection with the stream function-vorticity schemes[8]. In this paper we have considered an alternate way to utilize a consistent pressure equation in the formulation of consistently stabilized finite element methods. The regularization idea considered has been demonstrated to be useful especially when the rotational form of the Navier–Stokes system is used. An attraction of resulting schemes is that the performance is not very sensitive with respect to a choice of stabilization parameter. In the computational experiments the optimal orders of convergence were realized for large ranges of stabilization parameter and other problem or discretization parameter values.

The regularization strategy considered requires that the vorticity is treated as an auxiliary variable. This may seem as a significant computational burden compared to using

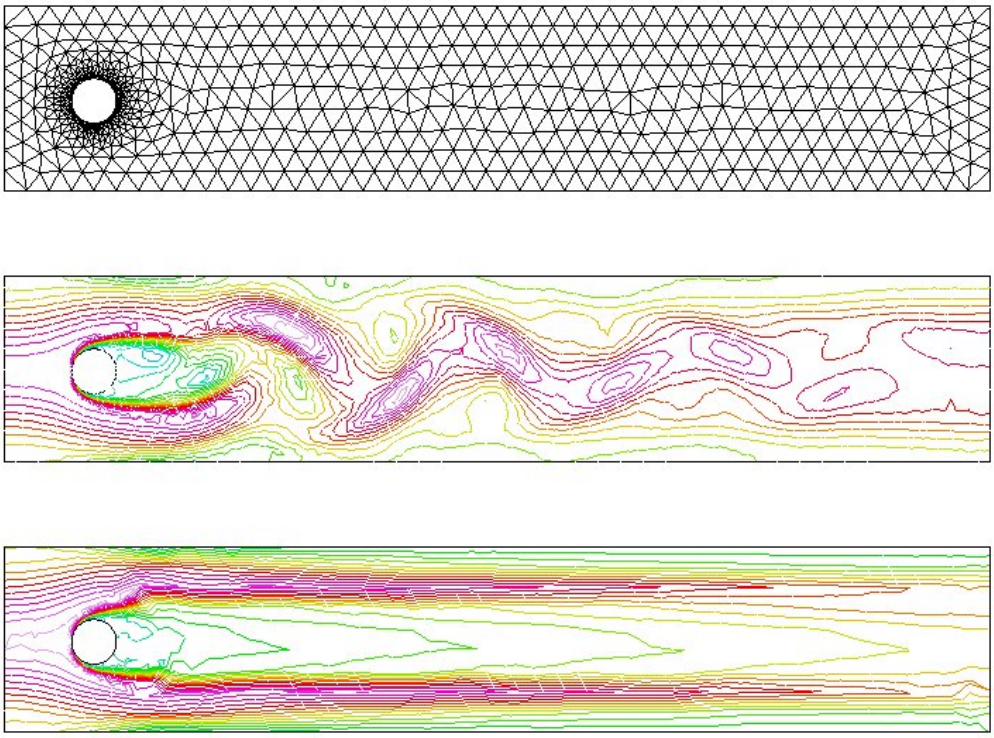

Figure 6: Contour plots of the total pressure approximation at $t = 5$ (s) on a coarse mesh displayed when the regularized scheme with $m = 2$ (middle) and the $P2P1$ discretization of the rotational form in the velocity and pressure variables (bottom) are employed. The $P2P1$ approximation fails to produce the von Karman vortex street, traces of which are visible in the case of the regularized discretization.

standard formulations in the velocity and pressure variables, in particular, when the equations are posed on a three-dimensional region. We note, however, that given a velocity the continuous vorticity approximation is here computed via the L^2 projection and efficient iterative methods for this subproblem are available. Therefore — given that the stabilization terms affect only the divergence-free constraint and that efficient methods for the vorticity computation exist — we expect that efficient block preconditioned solvers[2,9] developed in the context of standard velocity-pressure formulations may be extended to handle the linear systems arising here. We note that certain other stabilization strategies[10,11] similarly require handling an additional L^2 projection in order to evaluate the regularization terms.

REFERENCES

[1] P. M. Gresho and R. L. Sani, Incompressible Flow and the Finite Element Method: Volume 2: Isothermal Laminar Flow, *John Wiley* (1998).

[2] H. C. Elman, D. J. Silvester and A. J. Wathen, Finite Elements and Fast Iterative Solvers: with Applications in Incompressible Fluid Dynamics, *Oxford University Press* (2005).

[3] M. Braack, E. Burman, V. John and G. Lube, Stabilized finite element methods for the generalized Oseen problem, *Comput. Methods Appl. Mech. Engrg.*, **196**, 853-866 (2007).

[4] W. Layton, C. C. Manica, M. Neda, M. Olshanskii and L. G. Rebholz, On the accuracy of the rotation form in simulations of the Navier–Stokes equations, *J. Comput. Phys.*, **228**, 3433-3447 (2009).

[5] P. B. Bochev, M. D. Gunzburger and R. B. Lehoucq, On stabilized finite element methods for the Stokes problem in the small time-step limit, *Internat. J. Numer. Methods Fluids*, **53**, 573-597 (2007).

[6] M. Schäfer and S. Turek, Benchmark computations of laminar flow around a cylinder, In: E. H. Hirschel (Ed.), Notes on Numerical Fluid Mechanics, Vol. **52**, Vieweg, 547-566 (1996).

[7] J. L. Guermond, P. Minev and J. Shen, An overview of projection methods for incompressible flows, *Comput. Methods Appl. Mech. Engrg.*, **195**, 6011-6045 (2006).

[8] V. Girault and P.-A. Raviart, Finite Element Methods for Navier-Stokes Equations, *Springer Verlag* (1986).

[9] M. Benzi, G. H. Golub and J. Liesen, Numerical solution of saddle point problems, *Acta Numerica*, **14**, 1-137 (2005).

[10] K. E. Jansen, S. S. Collis, C. Whiting and F. Shakib, A better consistency for low-order stabilized finite element methods, *Comput. Methods Appl. Mech. Engrg.*, **174**, 153-170 (1999).

[11] P. Bochev and M. Gunzburger, An absolutely stable pressure-Poisson stabilized finite element method for the Stokes equations, *SIAM J. Numer. Anal.*, **42**, 1189 - 1207 (2004).